DRUG AND CHEMICAL TOXICOLOGY
2024, VOL. 47, NO. 6, 1018–1032
https://doi.org/10.1080/01480545.2024.2324332

Taylor & Francis
Taylor & Francis Group

RESEARCH ARTICLE

Beneficial effects of adipose-derived stromal vascular fraction on testicular injury caused by busulfan

E. Rumeysa Hekimoglu[a], Mukaddes Esrefoglu[a], Fatma Bedia Karakaya Cimen[a], Birsen Elibol[b], Huri Dedeakayogullari[c] and Özge Pasin[d]

[a]Department of Histology and Embryology, Faculty of Medicine, Bezmialem Vakıf University, Istanbul, Turkey; [b]Department of Medical Biology, Faculty of Medicine, Istanbul Medeniyet University, Istanbul, Turkey; [c]Department of Medical Biochemistry, Faculty of Medicine, Istinye University, Istanbul, Turkey; [d]Department of Biostatistics, Faculty of Medicine, Bezmialem Vakif University, Istanbul, Turkey

ABSTRACT

The use of stem cells can attenuate testicular injury and promote sperm production. The adipose-derived stromal vascular fraction (SVF) has become an attractive cell source for cell-based therapies. In this study, we aimed to investigate the therapeutic efficacy of SVF on busulfan-induced testicular damage in rats. Twenty-four male rats were randomly divided into control, busulfan, SVF, and busulfan + SVF groups. Testicular damage was induced by intraperitoneal administration of busulfan (35 mg/kg). SVF obtained from human adipose tissue using Lipocube SVF™ was injected into rats 5 weeks after busulfan administration. At the end of the 8th week, rats were sacrificed, and histopathological, biochemical, and western blotting analyses were performed. No harmful effects of SVF on healthy testis tissue and sperm parameters were detected. SVF improved busulfan-induced oxidative stress in both testis tissue and serum. SVF injection to damaged testicular tissue resulted in increases in the healthy spermatozoon numbers and decreases in the abnormal tail numbers. Additionally, SVF increased bax/Bcl, DAZL, and TGF-β1 levels whereas decreased ATG5 and NF-kB levels. According to the results we obtained in this study, we suggest that SVF is beneficial in restoring damaged tissue by primarily being a multipotent cell source, by inhibiting oxidative stress and converting necrotic cell death to apoptotic cell death. In the future, clinical applications should bring higher benefits. Since SVF is the patient's own tissue, being harmless, it will offer an advantageous supportive treatment option for patients already weakened by cancer and anticancer therapy.

ARTICLE HISTORY
Received 19 December 2023
Revised 23 February 2024
Accepted 23 February 2024

KEYWORDS
Busulfan; stromal vascular fraction; stem cell; infertility; testicular damage

1. Introduction

Spermatogenesis is a very vulnerable and complex process that eventually produces mature spermatozoa. Reduced fertility and infertility may result from several known and unknown variables influencing this process (Hosseını *et al*., 2014). For instance, anticancer medications used in greater quantities lead to poor spermatogenesis at increasing rates because the majority of anticancer agents cause infertility. That outcome leads to physical, psychological, social, and economic problems (Panahi *et al*., 2015).

Busulfan, chemically known as 1,4-butanediol dimethanesulfonate, has been used since 1959 as a chemotherapy drug. It is an alkylating agent that forms DNA–DNA inter-strand crosslinks between the DNA bases guanine and adenine and between guanine and guanine (Iwamoto *et al*., 2004) which prevents DNA replication. It not only prevents proliferation but also causes apoptosis in cells, which results in intra-strand DNA crosslinks that are irreversible by the body's repair mechanisms (Karstens & Krämer, 2007). Busulfan has various adverse effects on various systems including the male genital system. That injury is characterized by testicular damage and atrophy resulting in abnormalities in the morphology, motility, and number of spermatozoa (S. O. Abarikwu *et al*., 2022). Additionally, busulfan ultimately causes sterility by inhibiting cell division (S. O. Abarikwu *et al*., 2022; Intarapat *et al*., 2016). Busulfan-induced depletion of spermatogenic germ cells is generally reversible, albeit to varying degrees, and animals generally regain fertility due to the active re-proliferation of surviving germ cells (Choi *et al*., 2004).

In recent years, a great number of studies investigating the therapeutic effects of stem cell applications in various diseases have been published (Andia *et al*., 2019). Adipose-derived stem cells (ASCs) have become important tools in transplantation therapy to promote the healing of refractory wounds (Nourian Dehkordi *et al*., 2019), cartilage and bone regeneration (Pak *et al*., 2018; Roato *et al*., 2018), heart failure, and acute myocardial infarction, etc. (Gentile *et al*., 2017). For the isolation of ASCs, adipose tissue is separated by enzymatic and/or mechanical fragmentation, and at the end of this procedure, the stromal vascular fraction (SVF) is obtained. SVF

CONTACT E. Rumeysa Hekimoglu rumeysagurbuz@gmail.com Department of Histology and Embryology, Faculty of Medicine, Bezmialem Vakıf University, Fatih, Istanbul, Turkey
Supplemental data for this article can be accessed online at https://doi.org/10.1080/01480545.2024.2324332.

cell suspensions contain not only stem cells but also endothelial progenitor cells (EPCs), transitional cells, hematopoietic cells, pericytes, macrophages, fibroblasts, and supra-adventitial (SA) adipose stromal cells (ASCs) (Corselli *et al*., 2013; Guo *et al*., 2016). The number and proportion of cell subsets in SVF cell suspensions are analyzed through the detection of their specific cell surface markers such as EPCs; $CD45^{-}CD31^{+}CD34^{+}CD146^{+}$; ASCs; $CD45^{-}CD31^{-}CD13^{+}CD73^{+}$; transitional cells; $CD45^{-}CD31^{-}CD34^{+}CD146^{+}$; pericytes; $CD45^{-}CD31^{-}CD34^{-}$ $CD146^{+}$ (Corselli *et al*., 2013; Hager *et al*., 2013; Zimmerlin *et al*., 2013), anti-inflammatory M2 macrophages; $CD14^{+}$, $CD45^{+}$, $CD206^{+}$ (Eto *et al*., 2013) and SA-ASCs; $CD45^{-}CD31^{-}CD34^{+}CD146^{-}$ (Guo *et al*., 2016; Zimmerlin *et al*., 2013). In addition to various cell types, the suspensions also contain some growth factors including basic fibroblast growth factor (b-FGF), platelet-derived growth factor (PDGF), and insulin-like growth factor (IGF) (Grasys *et al*., 2016).

There have been several attempts to ameliorate busulfan-induced male sterility using natural products (S. Abarikwu *et al*., 2022; S. O. Abarikwu *et al*., 2022). A recent study demonstrated the protective effects of the adipose-derived SVF in severe acute ischemia injury of the rat testis (Andia *et al*., 2019; van Dongen *et al*., 2019; Zhou *et al*., 2019). Due to a limited number of studies related to the effects of SVF on chemotherapy-induced infertility, we aimed to study whether adipose-derived SVF has a protective effect on busulfan-induced testis damage in rats. In the future, clinical applications should bring higher benefits. Since SVF is the patient's own tissue, being harmless, it will offer an advantageous supportive treatment option for patients already weakened by cancer and anticancer agents.

2. Materials and methods

2.1. Isolation of SVF

Since a few experimental studies currently published reported no negative and harmful effects of human adipose tissue-derived SVF transferred to the rats (Cai *et al*., 2019; Harris *et al*., 2019; Yasuda *et al*., 2012), we injected human SVF to the testes of the rats. Briefly, human adipose tissue was aspirated from the abdomen of one female volunteer via standard vacuum-assisted liposuction (Lee *et al*., 2017). The volunteer was a healthy woman who underwent liposuction for weight loss, did not smoke or abuse alcohol, and had no chronic or sexually transmitted diseases. Written informed consent was obtained from the donor. The Ethics Committee of Bezmialem Vakif University Faculty of Medicine approved the study (2021/350). Mechanical digestion using Lipocube SVF™ was performed for SVF isolation from adipose tissue according to the protocol of Tiryaki *et al*. (2021).

2.2. Animals and study design

A total of 24 male Wistar Albino rats at the age of 11–12 weeks weighing 320–350 g were used in this study. All animals were obtained from the Experimental Animal Research Laboratory at Bezmialem Vakif University, Istanbul, Turkey. Ethical considerations were obtained from the Bezmialem Vakif University Ethics Committee (2021/168). Animals had free access to standard rat chow and water at controlled room temperature (22–25 °C) and humidity, on a 12-hour light/dark cycle for the duration of the study. The rats were randomly divided into the following four groups: control group (n = 6) (C; injection of dimethylsulfoxide (DMSO) intraperitoneally (i.p.)); busulfan group (n = 6) (BUS; injection of busulfan (i.p.) (Sigma, Cat: B2635, St. Louis, MO) at a single dose of 35 mg/kg in DMSO); SVF group (n = 6) (SVF; injection of a single dose SVF containing 1.2×10^6 cells into the mediastinum region of each testis) (Badawy *et al*., 2020; Cai *et al*., 2019); and busulfan + SVF group (n = 6) (BUS + SVF; 5 weeks after a single dose of 35 mg/kg busulfan injection, injection of SVF containing 1.2×10^6 a single dose cells into the mediastinum region of each testis). At the end of the 8th week, all rats were sacrificed under general anesthesia (80 mg/kg ketamine (Ketalar, Pfizer, Istanbul, Turkey) and 5 mg/kg xylase HCl (Rompun, Bayer, Istanbul, Turkey)).

2.3. Blood and tissue sampling

Blood samples were collected from the heart just before the sacrification. Serum was obtained by whole blood centrifugation (3000 × g, 20 min, at 4 °C) and stored at −80 °C until the analysis began. The semen was collected from the epididymis just before the sacrification. Just after the scarification, the abdominal cavity was exposed, and both testes were immediately removed. The right testes were fixed with Bouin's solution for histological analysis and the left testes were stored at −80 °C for the other analysis.

2.4. Sperm counting and morphological evaluation

The caudal part of the epididymis of rats in all groups was dissected into small pieces in Earle's balanced salts solution (Sigma, St. Louis, MO) for semen analysis. The mixture was precipitated, and the supernatant was removed. After that, the pellet was thinned with saline, and a 10 µm pellet was employed to count the spermatozoa in a Makler Counting Chamber (Sefi-Medical Instruments, Haifa, Israel) under a light microscope. Smears were prepared and stained with a Diff-Quick kit (Reagena-102164-Reastaınquıck-diff Kit, Toivala, Finland) for morphological assessment. About 100 spermatozoa were scored for head, neck, and tail morphology at ×400 magnification on a Nikon Eclipse i5 (Tokyo, Japan) microscope with Nikon DS-Fi1c camera attachment (Tokyo, Japan).

2.5. Histopathological analysis

For light microscopic and immunohistochemical evaluation, the right testes fixed in Bouin's solution were dehydrated in graded alcohols and embedded in paraffin. To provide optimizing tissue processing, a fully closed tissue processing device was used (TP 1020 Leica, New York, NY). The sections (3–5 µm in thickness) obtained from the paraffin blocks were stained with hematoxylin–eosin (H&E) and periodic acid-Schiff (PAS). Tubular damage scoring was done by two blind

observers separately according to the method of Esrefoglu M which was modified from Johnson's scoring (Gozen *et al*., 2013) (Table 1; Supplemental Figure 1). Ten successive areas across the cross-section of each sample were evaluated for degeneration degree under ×10 magnification. All samples were examined with a Nikon Eclipse i5 (Tokyo, Japan) microscope with Nikon DS-Fi1c camera attachment (Tokyo, Japan) and analyzed by NIS Elements version 4.0 image analysis system (Nikon Instruments Inc., Tokyo, Japan).

2.5.1. Immunohistochemical staining

Tissue sections were immunohistochemically stained by using the proliferating cell nuclear antigen (PCNA) polyclonal antibody (dilution: 1:1000, cat. no.: PA5-27214, Thermo Fisher, Waltham, MA), the deleted in azoospermia-like (DAZL) monoclonal antibody (dilution: 1:100, cat. no.: MA5-32708, Thermo Fisher, Waltham, MA), CD90 (Thy1) polyclonal antibody (dilution: 1:100, cat. no.: PA5-80127, Thermo Fisher, Waltham, MA), SensiTek HRP Anti-Polyvalent Lab Pack (cat. no.: SHP125, ScyTek Laboratories, Logan, UT) and ApopTag Plus Peroxidase In Situ Apoptosis Detection Kit (S7101, Millipore, Billerica, MA) for terminal deoxynucleotidyl transferase dUTP nick end labeling (TUNEL) method.

Table 1. Modified Johnson's scoring.

Score	Histologic findings
0	No pathological changes, intact, organized seminiferous epithelium
1	Mild degenerative changes/disorganization without vacuolization
2	Mild degenerative changes/disorganization with vacuolization
3	Moderate epithelial degeneration/disorganization without vacuolization
4	Moderate epithelial degeneration/disorganization with vacuolization
5	Severe epithelial degeneration/disorganization with vacuolization
6	Almost total epithelial loss with a few spermatogenetic cells/Sertoli cells

2.6. Western blotting method

Testis tissue of each rat was homogenized with 0.1 M phosphate-buffered saline (PBS) in a homogenizer using metallic beads. Then, homogenized tissues were centrifuged at 14 000 rpm for 15 min at 4 °C. The collected supernatants were used for sodium dodecyl sulfate-polyacrylamide gel electrophoresis (SDS-PAGE). Equal amounts of protein (40 µg/µl) that were determined with Pierce BCA Protein Assay Kit (Thermo Fisher Scientific, Waltham, MA) using Multiskan™ GO Microplate Spectrophotometer were diluted in sample buffer (Bio-Rad Laboratories, Inc., Hercules, CA), boiled for denaturation of proteins and loaded onto 4–20% Bis–Tris polyacrylamide gels and transferred into PVDF membranes using Bio-Rad protein electrophoresis and blotting system. Membranes were incubated in blocking solution (5% milk powder in 0.1% Tween 20/0.1 M Tris-buffered saline (TBST)) and immersed with primary antibodies (Bcl-2, Bax, NF-kB, phospho-p53 (Cell Signaling, Danvers, MA), ATG5 and TGF-β1 (Santa Cruz, Dallas, TX), DAZL (Invitrogen, Thermo Fisher Scientific, Waltham, MA), PCNA (Invitrogen, Thermo Fisher Scientific, Waltham, MA), and CD90 (Invitrogen, Thermo Fisher Scientific, Waltham, MA)). Each antibody was diluted in

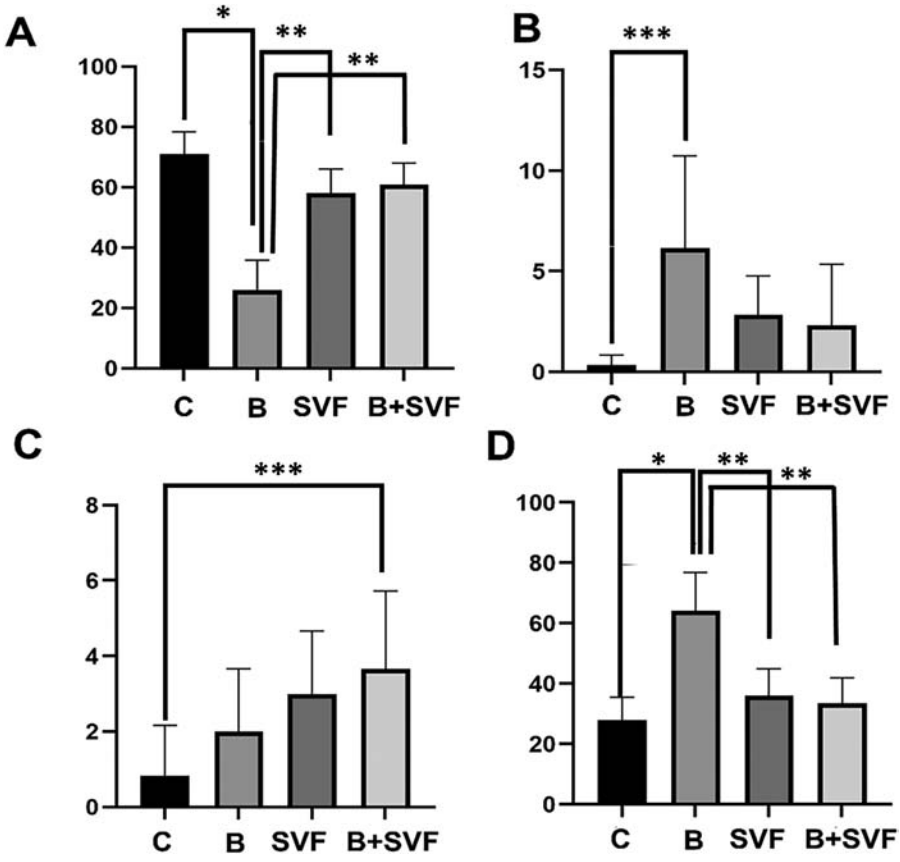

Figure 1. The mean numbers of healthy spermiums (A), abnormal heads (B), abnormal necks (C), and abnormal tails (D). *$p < 0.001$ vs. control group, **$p < 0.001$ vs. BUS group, and ***$p < 0.05$ vs. control group. C: control group; B: busulfan group; SVF: SVF group; B + SVF: busulfan + SVF group.

5% milk powder in 0.1% Tween 20/0.1 M TBST in a 1:1000 dilution and incubated with the membrane by shaking overnight. The following day, membranes were rinsed and incubated in peroxidase-coupled secondary antibodies which are diluted in the same solvent as the primary antibodies. Signal detection was made with luminol substrate (Advansta, San Francisco, CA) under a CCD camera with Fusion FX7 system (Vilber Lourmat, Marne-la-Vallée Cedex, France). Protein loading was controlled with a monoclonal mouse antibody against β-tubulin (Thermo Fisher Scientific, Paisley, UK). Immunoreactive protein bands were quantified densitometrically using the ImageJ analysis system (NIH, Seattle, WA).

2.7. Measurement of total antioxidant status (TAS) and total oxidant status

Serum TAS and TOS levels were determined with appropriate commercial kits (Rel Assay Diagnostics kit; Mega Tıp, Gaziantep, Turkey) developed by Erel (2004, 2005). The level of TAS and TOS was measured in blood serum samples and tissue homogenates at wavelengths of 240 nm and 520 nm, respectively, using a plate reader (Thermo Scientific Multiskan FC, 2011-06, Waltham, MA). For TAS measurements, Trolox, a water-soluble compound of vitamin E was used as a calibrator and the results were expressed as mmol. Trolox equivalent/l. For TOS measurements, H_2O_2 was used as the standard, and the results were expressed as μmol·H_2O_2 equivalent/l. The total protein amounts in homogenates were measured as above. Oxidative stress index (Iwamoto *et al.*, 2004) values were expressed as arbitrary units according to the following formula: OSI = (TOS (μmol·H_2O_2 equivalent/g protein)/TAS (mmol. Trolox equivalent/g protein)) × 100.

2.8. Statistical analysis

Descriptive statistics of the quantitative variables were given as mean, median, standard deviation, minimum, and maximum. The assumption about normal distribution was examined using the Kolmogorov–Smirnov test. The homogeneity of variances was investigated by the Levene test. If the assumption of homogeneity of variances was met, a one-way analysis of variance was used to compare the means of the groups. The Tukey test was used for *post hoc* pairwise comparisons. If the assumption of homogeneity of variances was not met but the normal distribution assumption was satisfied, the Brown–Forsythe test was used for group comparisons, and the Dunnett T3 test was used for *post hoc* pairwise comparisons. The Kruskal–Wallis test was used to compare the medians of the groups, and the Dunn test was used for *post hoc* comparisons. The statistical significance level was set at 0.05, and SPSS (version 26, IBM Corp., Armonk, NY) software was used for the calculations.

3. Results

3.1. Sperm analysis

Mean sperm counts of all rats among groups were similar. However, the mean healthy sperm number of the BUS group was lower than those of the control, SVF, and BUS + SVF groups ($p < 0.001$). Differences were detected in terms of the number of abnormal heads, necks, and tails. The mean abnormal head number of the BUS group was higher than that of the control group ($p < 0.05$). The mean abnormal tail number of the BUS group was higher than those of the control, SVF, and BUS + SVF groups ($p < 0.001$). SVF injection decreased the mean number of abnormal heads and tails without significant impact (Figure 1).

3.2. Histopathological changes

Histological features of the control group were quite normal except for rare intraepithelial and interstitial vacuolization derived from intratesticular DMSO injection (Figure 2(A)). Injected SVF area containing fat cells and heterogeneous cell groups was observed in the sections of the SVF group. A few atrophic tubules were observed around the SVF area (Figure 2(B)). Besides, intraepithelial and interstitial vacuolization was observed (Figure 2(C)). Tubular degeneration was obvious in the sections of the BUS group. Some tubules exhibited total atrophy/severe degeneration with vacuolization while others showed moderate or mild deterioration with or without vacuolization. Intertubular edema and vacuolization were also prominent (Figure 2(D)). Many tubules hosting a few spermatogenetic cells/Sertoli cells were devoid of the seminiferous epithelium (Figure 2(D,E)). Depending on the degree of degeneration, some spermatozoa or spermatids were observed in the tubule lumens (Figure 2(E)). Epithelial desquamation was also detected (Figure 2(F)). Injected SVF area containing fat cells and heterogeneous cell groups was observed in the sections of the BUS + SVF group as observed in the sections of the SVF group. A few atrophic tubules were detected around the SVF area (Figure 1(G)). Tubular degeneration was observed with mostly mild to moderate degrees. Rarely complete atrophy and severe degeneration were detected. Intraepithelial vacuolization and interstitial edema and vacuolization were still obvious (Figure 2(G,H)).

Basal lamina surrounding each tubule of the control and SVF groups was even (Figure 3(A,B); respectively). The tubular basal lamina of the BUS and BUS + SVF groups was not generally even, thinner, or thicker than expected (Figure 3(C,D); respectively).

3.3. Histopathological degeneration scores

The outcomes of the grading method that Esrefoglu M adjusted agreed with the findings of the microscopical observations. Some significant differences were detected in terms of the mean histopathological degeneration score (MHDS) of the groups. The MHDS of the control group was found to be significantly lower than the mean of the BUS and BUS + SVF groups ($p < 0.001$; $p = 0.006$). The MHDS of the SVF group was significantly lower than the BUS group ($p = 0.005$). The MHDS of the BUS + SVF group was (3.32 ± 1.34) lower than that of the BUS group (4.78 ± 0.82) although statistically insignificant.

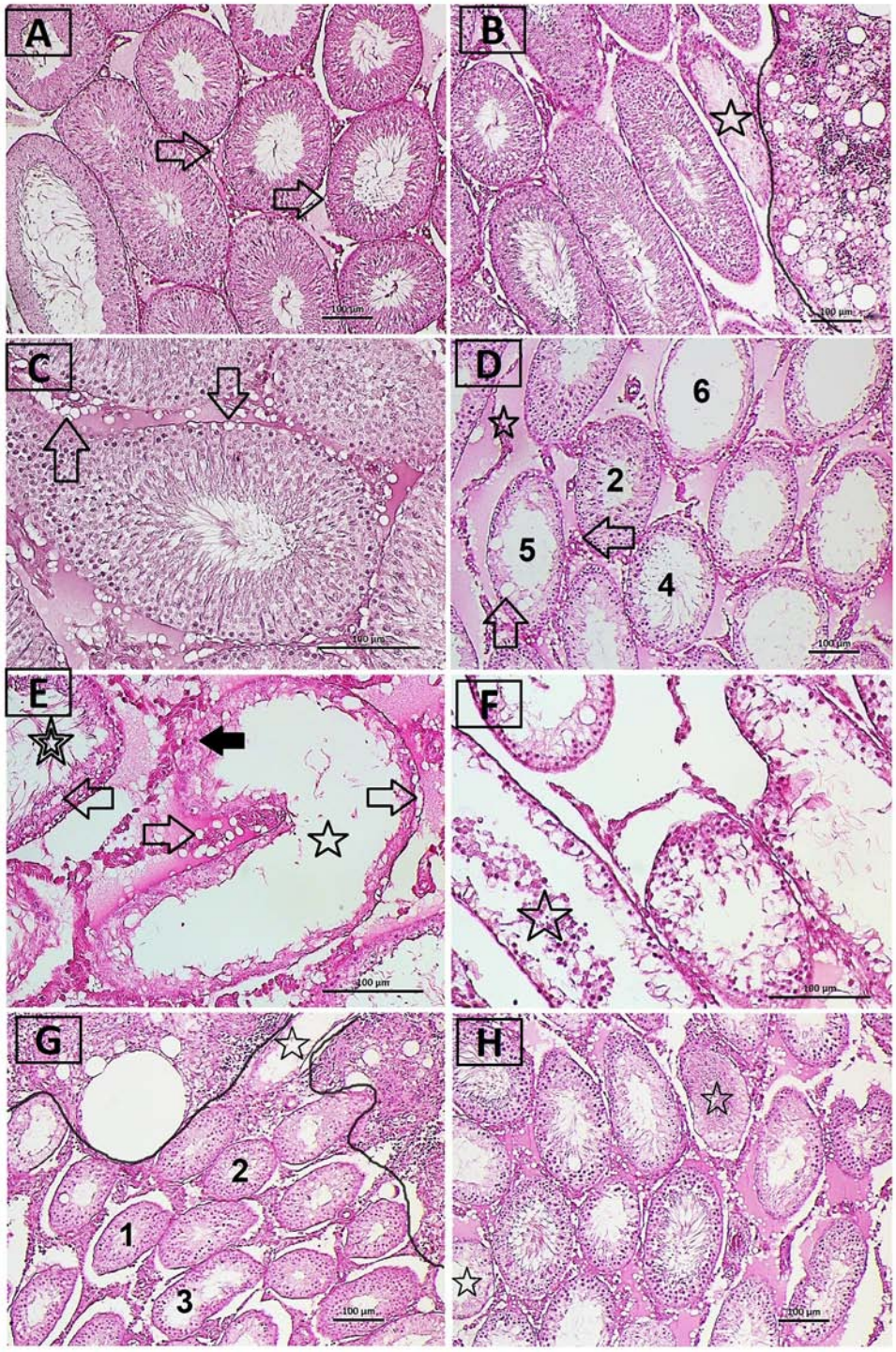

Figure 2. Histopathological features of hematoxylin and eosin-stained testis tissue of all groups. A: control group. Normal in histological appearance except for a few vacuoles within the epithelium and interstitial tissue (arrows). (B, C) SVF group. (B) SVF (stromal vascular fraction) area containing fat cells and heterogeneous cell groups is observed at the right side of the figure. An atrophic tubule is marked by an asterisk. (C) Intraepithelial and interstitial vacuolization are observed (arrows). (D–F) Busulfan group. (D) Tubular degeneration and intertubular edema (asterisk), intraepithelial, and interstitial vacuolization (arrows) are obvious. Tubules reveal total atrophy (6), severe degeneration with vacuolization (5), moderate degeneration with vacuolization (4), or mild degeneration with vacuolization (2). (E) An atrophic tubule (asterisk) with a few cells (black arrows) and another moderately degenerated tubule containing sperms and spermatids (double asterisk) are seen. Intratubular and intertubular vacuolization are marked (arrows). (F) Epithelial desquamation is obvious (asterisk) in addition to degeneration. (G, H) Busulfan + SVF group. (G) SVF area containing fat cells and heterogeneous cell groups is observed at the upper half of the figure. An atrophic tubule next to that area is marked by an asterisk. Tubules revealing mild degenerative changes without vacuolization (1), with vacuolization (2), and moderate degenerative changes without vacuolization (3) are marked. (H) Two atrophic tubules are marked with asterisks. The other tubules show mild to moderate degenerative changes with or without vacuolization. Intraepithelial vacuolization and interstitial edema and vacuolization are obvious.

3.4. Immunohistochemical analysis results

PCNA, CD90, and DAZL immunohistochemistry were applied to the paraffin sections of the groups. The mean PCNA-positive epithelial cell number of the tubules of the control group was 87 ± 8.14, that of the SVF group was 76.75 ± 3.15, that of the BUS group was 57.12 ± 15.68, and finally, that of the BUS + SVF

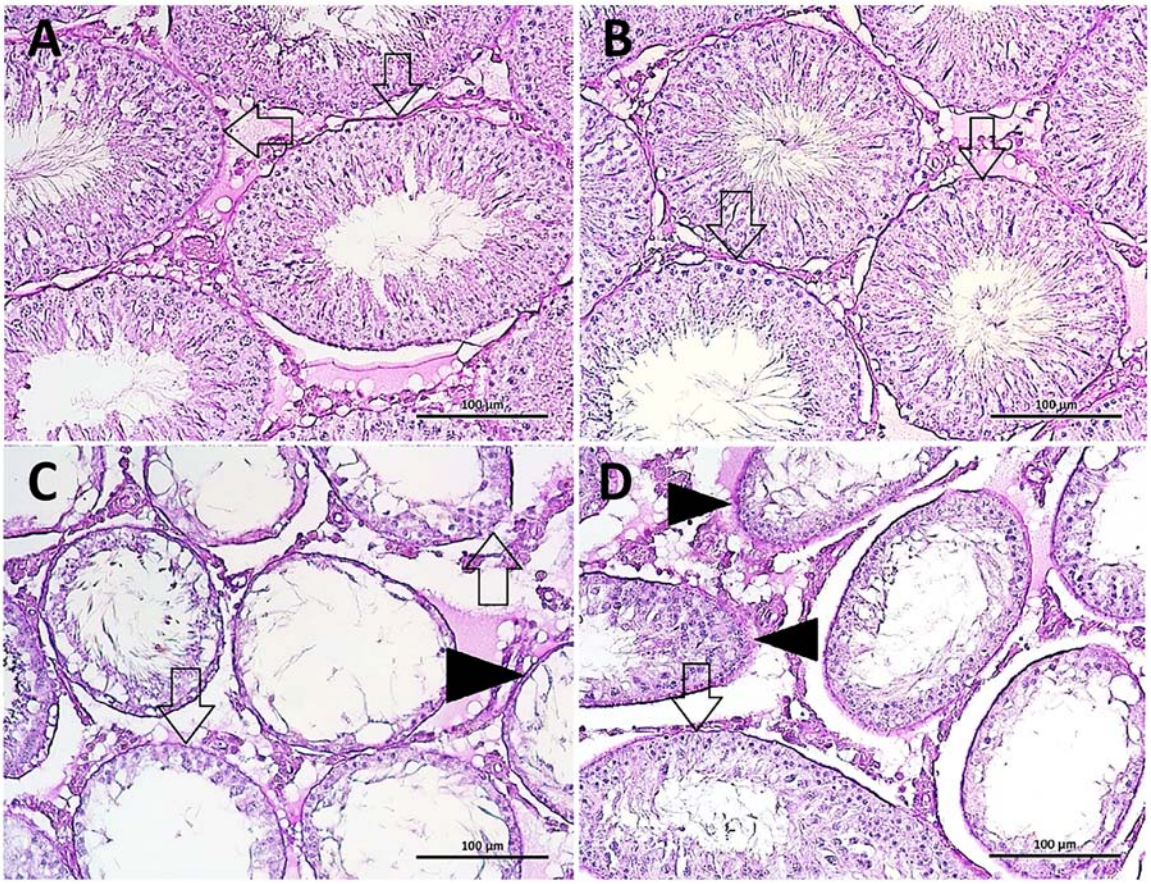

Figure 3. The PAS (periodic acid-Schiff) positive stained tubular basal lamina of the groups. (A) Control group. Normal in histological appearance, basal lamina evenly surrounds the tubules (arrows). (B) SVF group. Normal in histological appearance, basal lamina evenly surrounds the tubules (arrows). (C) Busulfan group. The basal lamina is generally thinner (arrow) or thicker (black arrowhead) than expected. (D) Busulfan + SVF group. The basal lamina is generally thinner (arrow) or thicker (black arrowhead) than expected.

group was 73.2 ± 6.14. A significant difference was detected between the control and BUS groups ($p < 0.005$) (Figure 4). The lowest mean TUNEL + cell number was detected in the control group whereas the highest one was detected in the BUS group. The mean numbers of TUNEL + cells of the BUS and BUS + SVF groups were higher than that of the control group ($p < 0.001$, $p < 0.05$; respectively). Additionally, the mean number of TUNEL + cells of the BUS group was higher than that of the SVF group ($p < 0.05$) (Figure 5). CD90-positive staining was detected in some cells of the injected SVF mass, some cells between tubules, rarely within the tubule epithelium, endothelial cells, and blood cells in the lumen. Immunoreactivity was detected in endothelial cells and blood cells. A few reactive cells were observed in the interstitial tissue but not within the epithelium in the control group (Figure 6(A)). There were many positively stained cells in the injected SVF mass and relatively higher numbers of immunoreactive cells in the interstitial tissue in the SVF group. Vascular staining was valid (Figure 6(B,C)). In the BUS group, some positively stained cells were detected in the interstitial tissue, peritubular tissue, and within the epithelium. Vascular positivity was clear (Figure 6(D,E)). There were many positively stained cells in the injected SVF mass and relatively higher numbers of immunoreactive cells in the interstitial tissue in the BUS + SVF group. Some positively stained cells were detected in the interstitial tissue, peritubular tissue, and within the epithelium. Vascular positivity was obvious (Figure 6(F)). DAZL-positive cells were detected within the seminiferous epithelium of the control group. Immunoreactive staining was observed in the cytoplasm of spermatogonium and spermatocytes but primarily in the nuclei of spermatids (Figure 7(A)). Immunoreactive staining cells were detected in the injected SVF mass in the SVF group (Figure 7(B)). Strong immunoreactivity was observed in the nuclei of spermatogonia, primary spermatocytes, and spermatids (Figure 7(C)). Positive staining was not detected in fully atrophic tubules in the BUS group. In the case of the existence of the seminiferous epithelium, immunoreactivity was generally limited to the basal half of the seminiferous epithelium because of the damage, disorganization, and loss of the spermatids (Figure 7(D,E)). Immunoreactive staining cells were detected in the injected SVF mass in the BUS + SVF group. Besides immunoreactivity was generally limited to the basal half of the seminiferous epithelium because of the damage, disorganization, and loss of the spermatids. Immunoreactivity was naturally absent in fully atrophic tubules (Figure 7(F)).

3.5. Western blotting-analysis results

The lowest tissue bax/Bcl2 level (apoptotic index) was detected in the SVF group whereas the highest bax/Bcl2 level

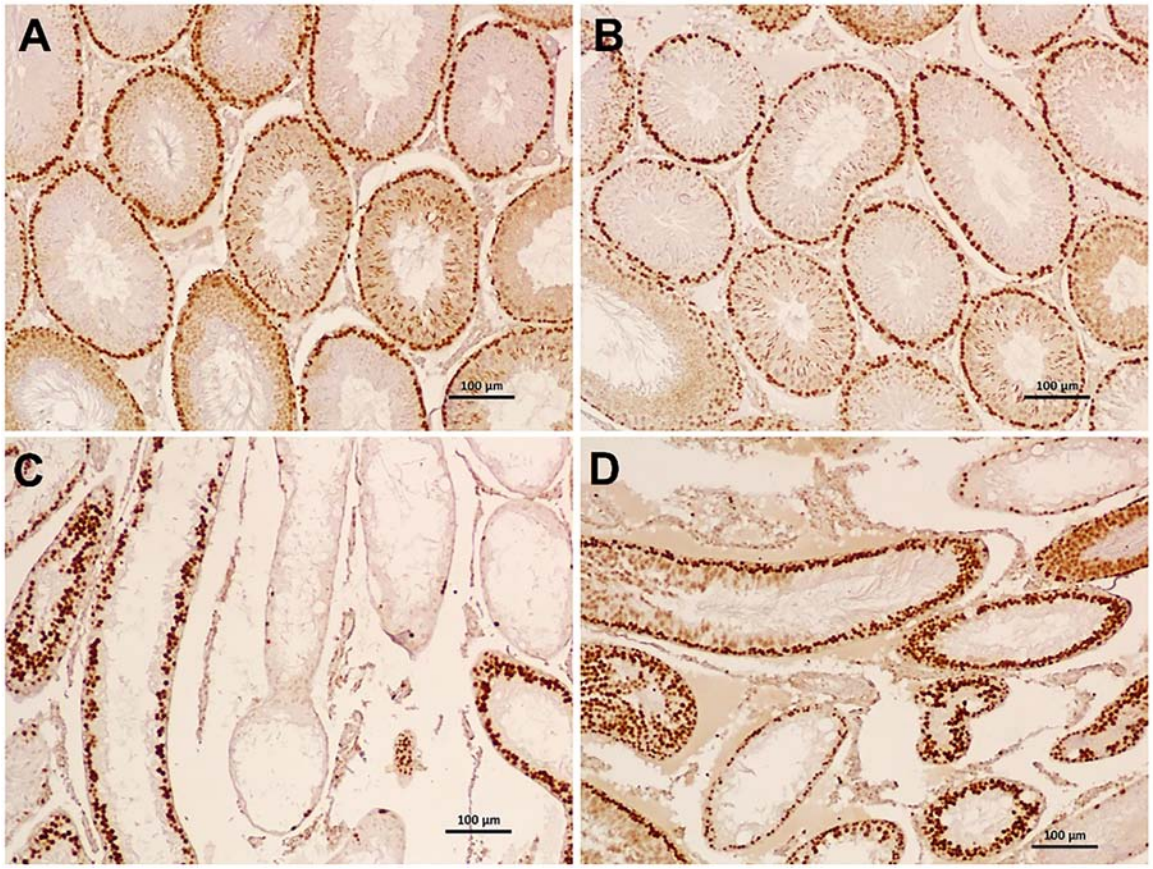

Figure 4. PCNA + cell distribution of the control (A), SVF (B), BUS (C), and BUS + SVF (D) groups, respectively. PCNA immunohistochemical technique.

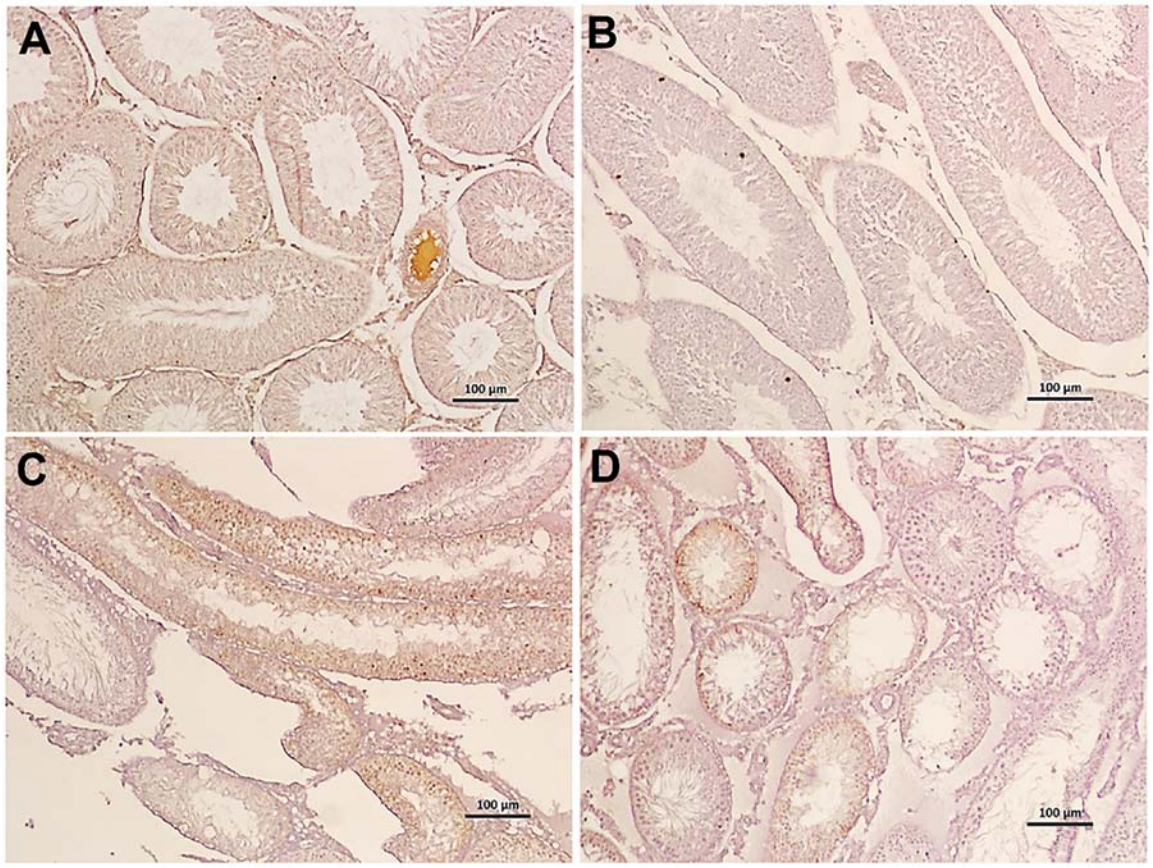

Figure 5. TUNEL + cell distribution of the control (A), SVF (B), BUS (C), and BUS + SVF (D) groups, respectively. TUNEL immunohistochemical technique.

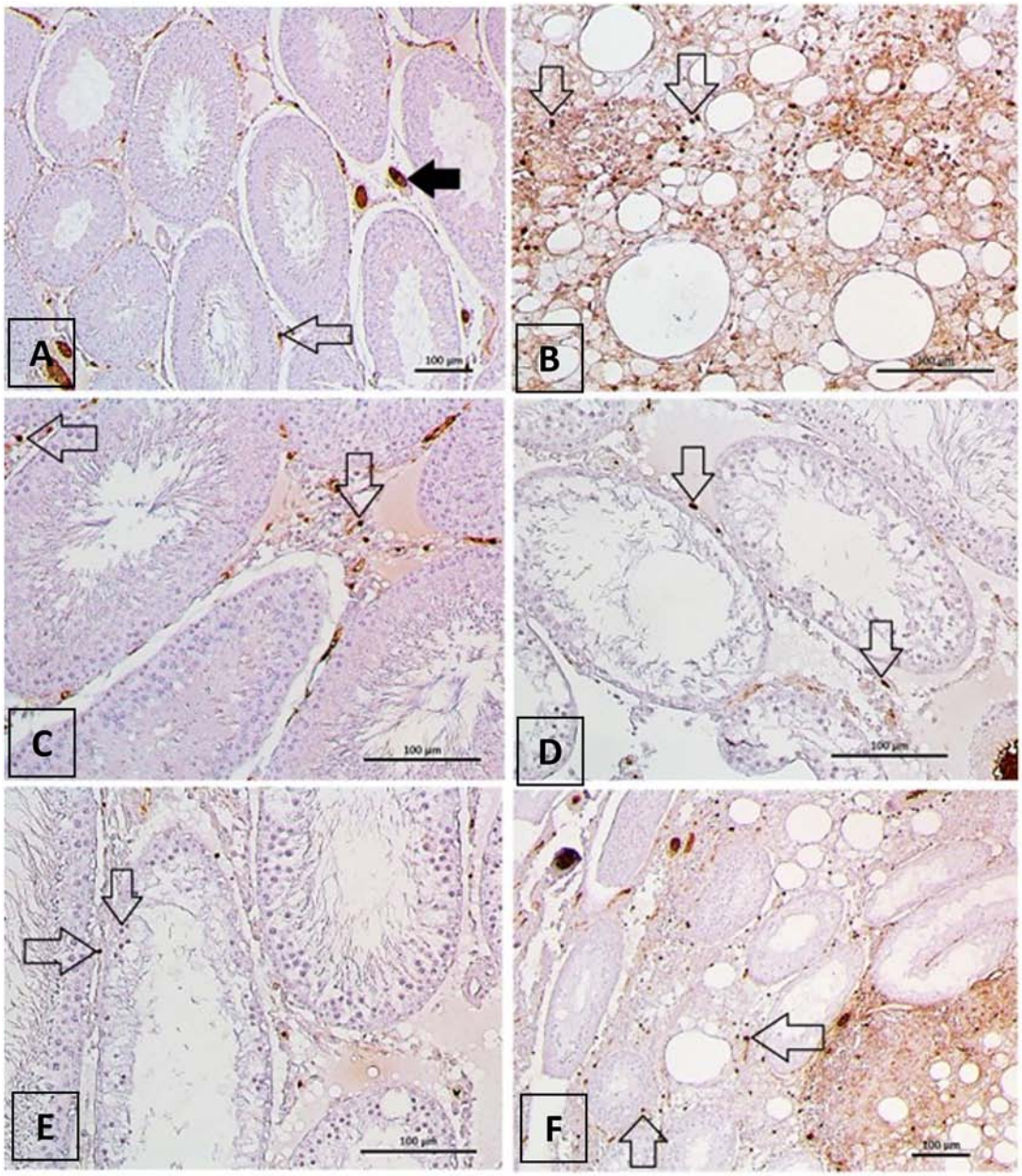

Figure 6. CD90 immunoreactivity of the groups. (A) Control group. A few reactive cells are observed in the interstitial tissue (arrow). Vascular reactivity is clear (black arrow). (B, C) SVF group. (B) Many positively stained cells in the injected SVF (stromal vascular fraction) mass are detected (arrow). (C) Relatively higher numbers of immunoreactive cells in the interstitial tissue are observed (arrows). (D, E) BUS group. (D) Some positively stained cells are detected in the interstitial tissue (arrows). Vascular positivity is obvious. (E) Some positively stained cells are detected in the peritubular tissue and within the epithelium (arrows). (F) BUS + SVF group. Many positively stained cells in the injected SVF (stromal vascular fraction) mass, in the interstitial tissue, and in the epithelium (arrows). Vascular positivity is obvious.

was detected in the BUS + SVF group. The bax–Bcl-2 level of the BUS group was higher than that of the control group, whereas lower than that of the BUS + SVF group ($p < 0.001$). Statistical differences were detected between the BUS + SVF and the control, the BUS + SVF, and SVF, and additionally between the BUS and SVF groups ($p < 0.001$; for all) (Figure 8(A)). The CD-90 level was increased in the BUS group compared to that of the control group ($p < 0.05$), SVF group ($p < 0.005$), and the BUS + SVF group ($p < 0.001$) (Figure 8(B)). The DAZL levels did not change due to BUS injection vs. the control group; however, SVF injection to both healthy and diseased testes increased the levels of DAZL vs. the control group ($p < 0.001$; for both) (Figure 8(C)). The phosphorylated p53 level was significantly increased in the BUS vs. the control group ($p < 0.05$), and in the SVF group vs. the control group ($p < 0.001$). p53 level of BUS + SVF group was decreased vs. the SVF group ($p < 0.05$), whereas increased vs. control group ($p < 0.05$) (Figure 8(D)). The tissue ATG5 levels were significantly increased in the BUS group and in the SVF group compared to that of the control group ($p < 0.005$, $p < 0.05$; respectively). ATG5 level of the BUS + SVF group was decreased vs. the BUS group ($p < 0.001$) (Figure 8(E)). The level of TGF-β1 was not changed due to BUS injection; however, TGF-β1 levels of SVF and BUS + SVF groups were

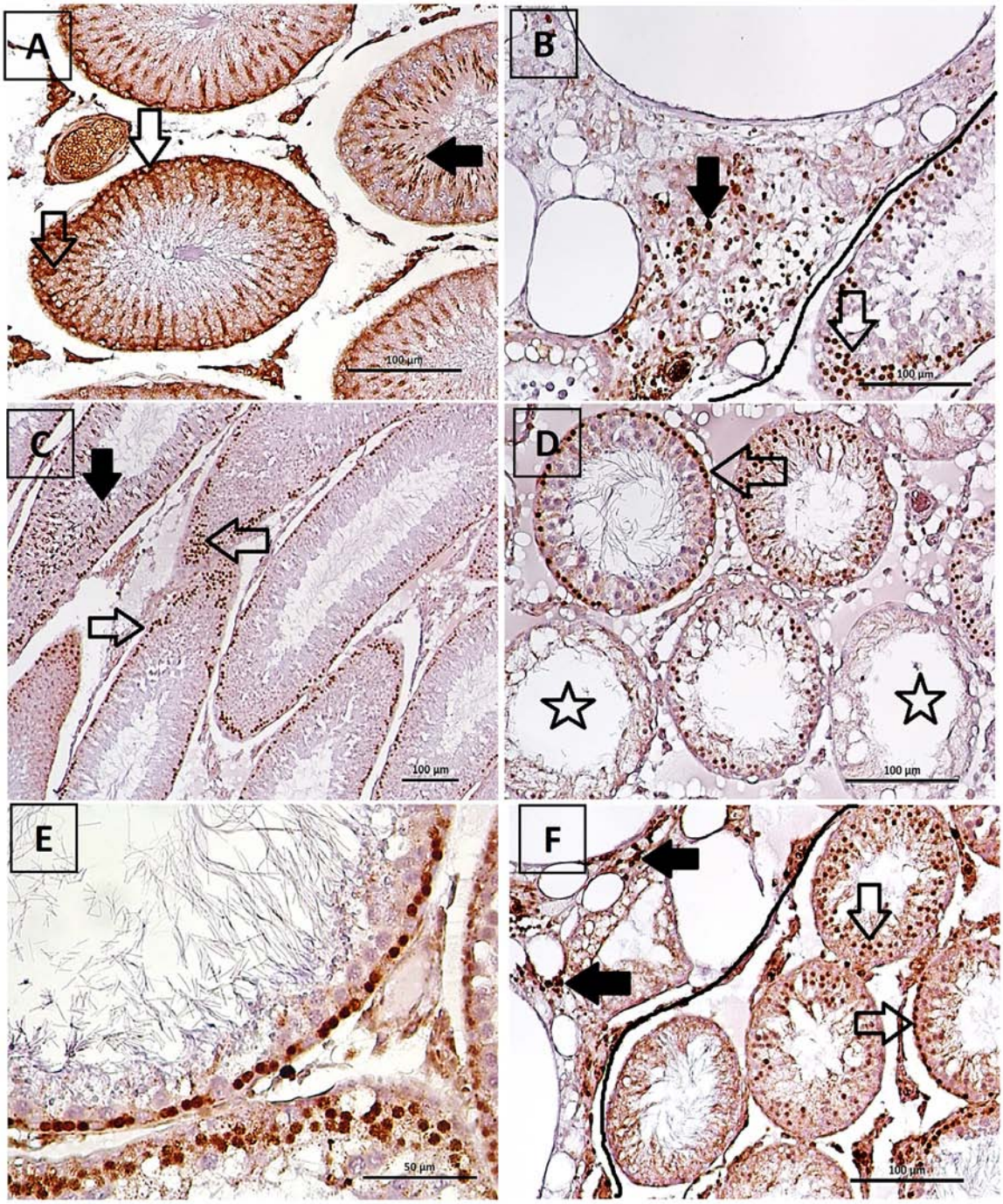

Figure 7. DAZL (deleted in azoospermia-like) immunoreactivity of the groups. (A) Control group. DAZL (deleted in azoospermia-like)-positive immunoreaction is obvious primarily in the cytoplasm of spermatogonium and spermatocytes (arrows) but primarily in the nuclei of spermatids (black arrow). (B, C) SVF group. (B) Immunoreactive staining nuclei in the injected SVF (stromal vascular fraction) mass (left side of the black line) (black arrow) and seminiferous epithelium are marked (arrow). (C) Strong immunoreactivity is detected in the nuclei of spermatogonia, primary spermatocytes (arrow), and spermatids (black arrow). (D, E) BUS group. (D) Positive staining is not detected in fully atrophic tubules (asterisks). In the case of the existence of the seminiferous epithelium, immunoreactivity is limited to the basal half of the seminiferous epithelium (arrow). (E) Positive staining is observed in the nuclei of the spermatogonia and primary spermatids. (F) BUS + SVF group. Immunoreactive staining nuclei in the injected SVF (stromal vascular fraction) mass (left side of the black line) (black arrows) and seminiferous epithelium (arrows) are marked.

increased compared to those of the control and BUS groups ($p < 0.05$ and $p < 0.001$, respectively) (Figure 8(F)). Finally, NF-kB level was significantly increased in the BUS group vs. the control group ($p < 0.05$). SVF injection significantly decreased that level compared to the BUS group ($p < 0.001$). The NF-kB level of the BUS + SVF group was lower than that of the BUS group ($p < 0.001$) (Figure 8(G)).

3.6. Oxidative stress parameters

TOS and TAS levels of testis tissues and serum were measured; OSIs were calculated (Figure 9). The tissue TOS level of the BUS group (10.32 ± 1.65) was higher than those of the control (8.87 ± 0.10), SVF (7.96 ± 0.58; $p < 0.001$), and BUS + SVF (9.54 ± 0.41) groups. The lowest tissue TOS level

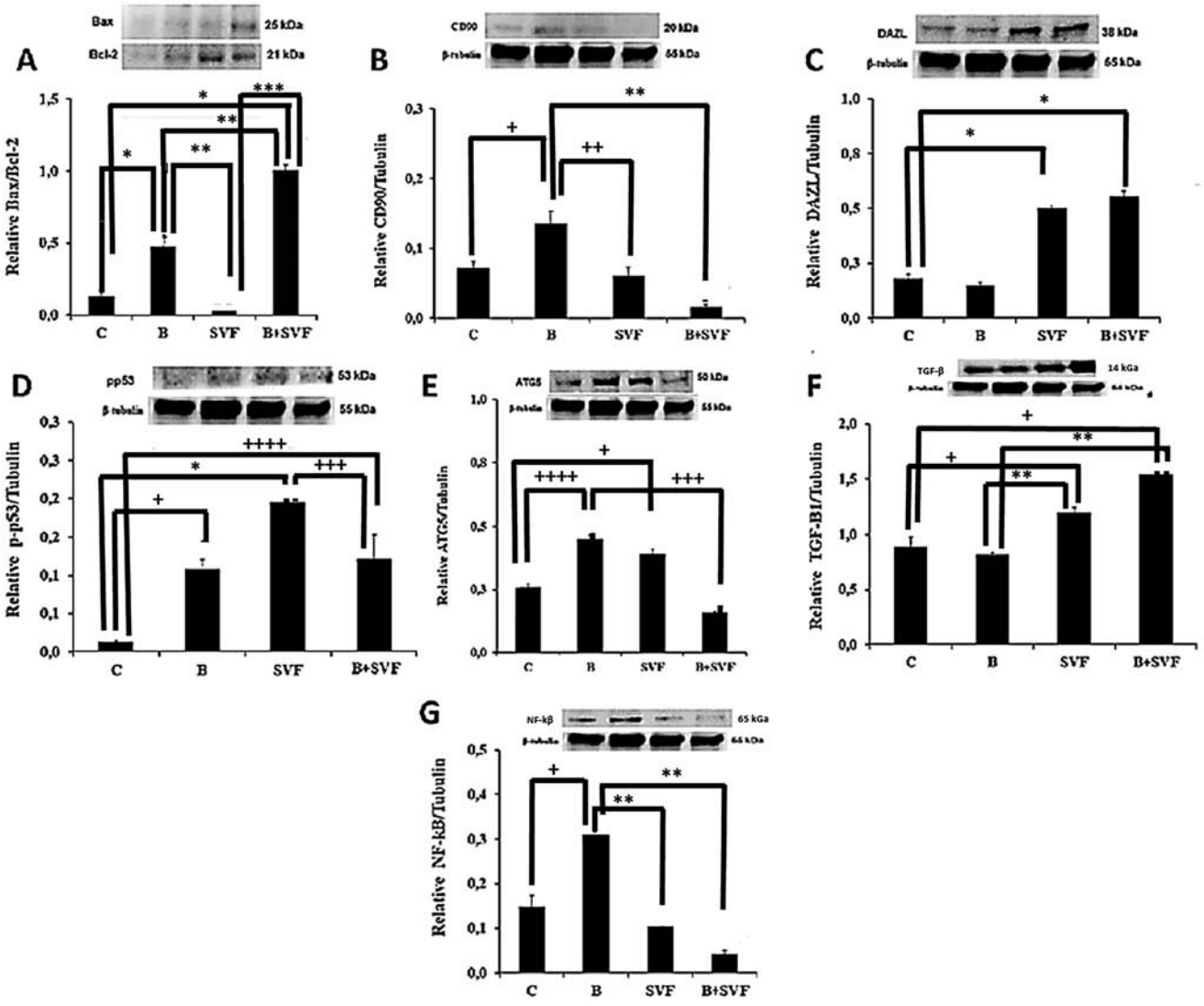

Figure 8. Tissue levels of bax–Bcl-2 (A), CD90/tubulin (B), DAZL/tubulin (C), pp53/tubulin (D), ATG5/tubulin (E), TGF-β1/tubulin (F), and NF-kB/tubulin (G) are shown. *$p < 0.001$ vs. control group, **$p < 0.001$ vs. BUS group, ***$p < 0.001$ vs. SVF group, $^{+}p < 0.05$ vs. control group, $^{++}p < 0.005$ vs. BUS group, $^{+++}p < 0.05$ vs. SVF group, and $^{++++}p < 0.005$ vs. control group. C: control group; (B) busulfan group; SVF: SVF group; B + SVF: busulfan + SVF group.

was detected in the SVF group vs. the control ($p = 0.05$), BUS ($p < 0.001$), and BUS + SVF ($p < 0.001$) groups. Similarly, the serum TOS level of the BUS group (11.12 ± 0.85) was higher than those of the control (9.46 ± 0.35; $p < 0.05$), SVF (8.17 ± 0.16; $p = 0.001$), and BUS + SVF (8.77 ± 0.56; $p < 0.005$) groups. Additionally, the serum TOS level of the SVF group was even lower than that of the control group ($p < 0.001$). The lowest tissue TAS level was detected in the BUS group (0.63 ± 0.09) vs. the control (0.95 ± 0.07; $p < 0.005$), SVF (0.92 ± 0.07; $p < 0.005$), and BUS + SVF (0.95 ± 0.07; $p < 0.005$). Similarly, the lowest serum TAS level was detected in the BUS group (0.74 ± 0.02) vs. the control (0.92 ± 0.05; $p \leq 0{,}001$), SVF (1.03 ± 0.17; $p < 0.05$), and BUS + SVF groups (0.83 ± 0.06). The highest serum TAS level was detected in the SVF group. The highest tissue and serum OSI were detected in the BUS group. Statistical differences were detected between the BUS and control ($p < 0.05$), SVF ($p < 0.005$), and BUS + SVF ($p < 0.05$) in terms of tissue OSIs. Statistical differences were detected between the BUS and control ($p \leq 0.001$), SVF ($p \leq 0.001$), and BUS + SVF ($p \leq 0.001$) in terms of serum OSIs.

4. Discussion

A major hindrance to the medical application of chemotherapy medications is the considerable destruction of germ cells, leading to infertility among the patients who have survived cancer chemotherapy. Busulfan, a popular anticancer drug, has extremely significant negative effects on male reproductive system, thus fertility maintenance during busulfan treatment is seriously concerned. Adverse effects of busulfan on the male genital system were characterized by testicular damage and atrophy resulting in abnormalities in the morphology, motility, and number of spermatozoa (S. O. Abarikwu *et al.*, 2022). In rodents, busulfan has been reported to be responsible for sterility stemming from spermatogonial cells (Anjam *et al.*, 2007; Benavides-Garcia *et al.*, 2015). Busulfan may elicit a variety of biological processes, including cytotoxicity, ROS-induced apoptotic cell death, and autophagy (Vahdati *et al.*, 2015; Xu *et al.*, 2016). Additionally, it has been reported to reduce serum testosterone levels, total antioxidant capacity, gene expression of Bcl2, and the number of

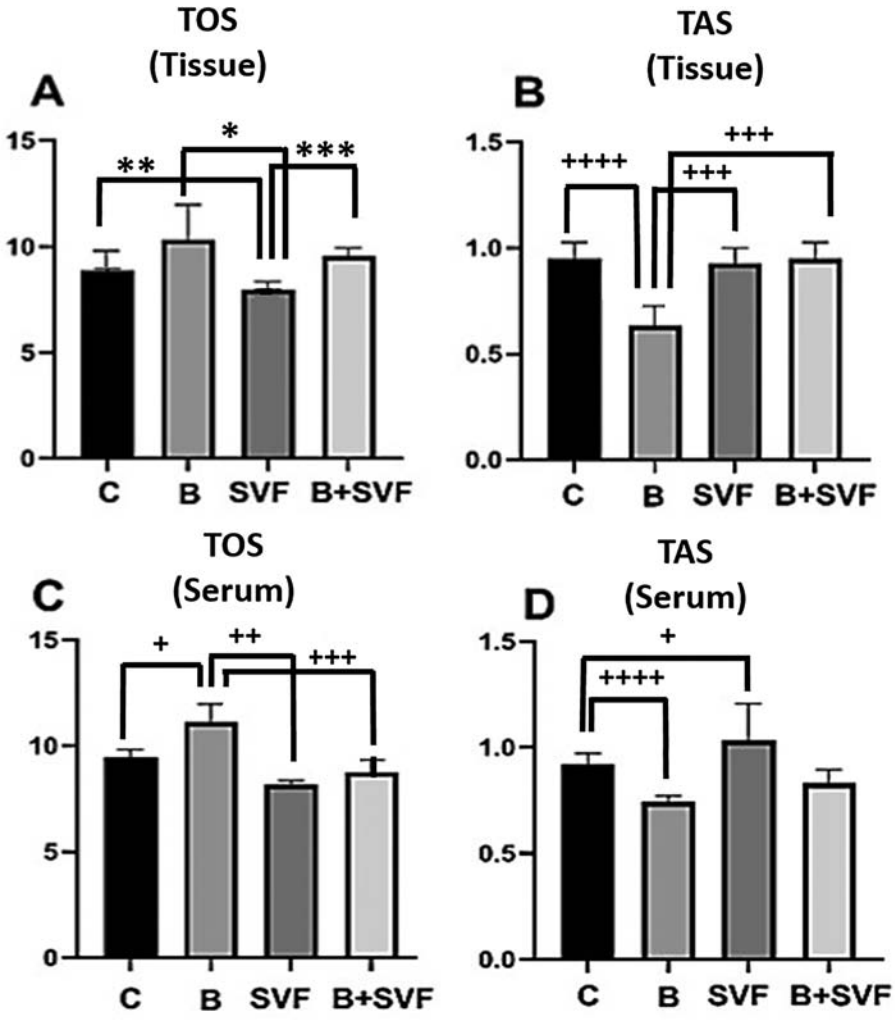

Figure 9. Tissue and serum levels of TOS (A, C; respectively) and tissue and serum TAS levels (B, D; respectively) of the groups are shown. *$p < 0.001$ vs. BUS group, **$p = 0.05$ vs. control group, ***$p < 0.001$ vs. SVF group, $^{+}p < 0.05$ vs. control group, $^{++}p = 0.001$ vs. BUS group, $^{+++}p < 0.005$ vs. BUS group, and $^{++++}p < 0.005$ vs. control group.

spermatogonia, spermatocyte, spermatid, Sertoli cells, and Leydig cells (Rostami *et al*., 2022). In the present study, oxidative stress parameters, TOS, TAS, and calculated OSI, measured in the testis tissue and serum supported that oxidative stress, which is caused by increased reactive oxygen species (ROS) and decreased antioxidant enzymes, plays an important role in the pathogenesis of busulfan-induced organ damage. In the BUS group, the increase of the NF-kB level, which is the main regulator of oxidative stress and inflammatory response, may also support the increased generation of ROS due to busulfan treatment (Oliveira-Marques *et al*., 2009; Raish *et al*., 2018). Several studies emphasize oxidative stress-induced cell death resulting in tissue damage in busulfan-treated rodents (Nasimi *et al*., 2018; Qian *et al*., 2020; Rostami *et al*., 2022). In the present study, testicular damage characterized by seminiferous tubule atrophy and degeneration, increased apoptosis parameters, impaired sperm parameters, and increased oxidative stress parameters indicated the toxic effects of busulfan. In addition to degeneration and atrophy, intraepithelial and intertubular vacuolization and intertubular edema were obvious. Some tubules showed moderate or mild deterioration with or without vacuolization. Many tubules hosting a few spermatogenetic cells/Sertoli cells were devoid of the seminiferous epithelium. Depending on the degree of degeneration, a few to some spermatozoa or spermatids were observed in the lumens. The anticipated pattern of busulfan-induced testicular injury has been shown by numerous researchers (Harris *et al*., 2019; Yasuda *et al*., 2012). Semen analysis revealed a decrease in terms of the healthy spermatozoon number but an increase in the number of spermatozoa having an abnormal head and tail in the BUS group. The healthy and damaged spermatozoon numbers were consistent with the changes in terms of survived or damaged tubule numbers in the BUS group.

In the present study, busulfan treatment resulted in a significant increase in TUNEL + cell numbers and the bax–Bcl-2 levels compared to the control group. Various studies emphasize busulfan-induced apoptotic cell death in addition to necrotic cell death (Nasimi *et al*., 2018; Qian *et al*., 2020; Rostami *et al*., 2022; Taslidere *et al*., 2022). On the contrary, busulfan suppressed the proliferation rate of spermatogenetic cells ($p < 0.005$) as various researchers have reported (Qian *et al*., 2020; Rostami *et al*., 2022; Taslidere *et al*., 2022). The relative increase in the phosphorylated p53 level in the BUS

group also indicates the increased molecular role of p53 inducing apoptotic effector protein bax to trigger apoptosis (Rufini *et al*., 2013; Speidel, 2015). Several different types of DNA damage can activate p53 as a transcription factor. Activation of p53 can lead to either cell cycle arrest and DNA repair or apoptosis (Pieri *et al*., 2017). On the other hand, in the BUS group significantly higher levels of ATG5, which is one of the autophagy-related proteins, showed that busulfan stimulated the autophagy. Autophagy is a natural, destructive cellular mechanism involving the degradation of cellular components through lysosomal machinery, thus maintaining cellular homeostasis and supplying substrates for energy generation (González *et al*., 2018). Increased levels of ATG5 might be an indicator of busulfan-induced organelle damage. Despite the highest cell death and lowest cell proliferation, the highest CD90 level was detected in the BUS group. Consistently, CD90 positivity was obvious in the sections obtained from the BUS group. CD90 (i.e., THY1) is a glycoprotein known as a mesenchymal stem cell (MSC) marker that is expressed in various cell types including male and female gonadal cells (Lin *et al*., 2013). We suggest that CD90+ stem cells are migrated, proliferated, and activated at the highest rates following an injury in order to replace the damaged cells.

Stem cell therapy promises to be a possible source of male and female germ cells in cases of infertility and sterility (Drusenheimer *et al*., 2007; Nayernia *et al*., 2006). Previous studies have shown that stem cells injection into the testicular tissue provides a useful strategy for the treatment of infertility (Hsiao *et al*., 2015; Mehrabani *et al*., 2015). Since bone marrow-derived MSCs need more time and effort to separate, adipose tissue-derived stem cells in SVF have been the favored option in stem cell transplantation therapies (Corselli *et al*., 2013; Eto *et al*., 2013; Hager *et al*., 2013). SVF cell suspensions contain not only MSCs but also EPCs, transitional cells, hematopoietic cells, pericytes, macrophages, fibroblasts, and SA ASCs (Guo *et al*., 2016; Zimmerlin *et al*., 2013). Due to the presence of the blood–testis barrier, systemically administered stem cells coming through the circulation may not be able to penetrate the organ. Thus, the current favored technique involves injecting stem cell containing fluid or tissue into the testicular tissue. Besides it is not necessary to avoid to perform inter-species trials since human ASCs do not express MHC class-II they will not trigger a xenogenic immunological reaction (Siregar *et al*., 2021).

In the present study, injected SVF area containing fat cells and heterogeneous cell groups was observed in the sections of SVF and BUS + SVF groups. Immunohistochemistry revealed that some of the members of the heterogeneous cell groups were CD90+ stem cells. Many CD90+ cells were detected in the injected SVF mass, in the interstitial tissue, and at the vascular wall. Some of those cells were located within the seminiferous epithelium in the BUS + SVF group. Stem cells injected in SVF mass can disperse into the interstitial tissue and reach the damaged tissue. Any agent applied for therapeutic purposes principally must not cause any morphological or functional harm to the tissue. In the present study, SVF alone has not significantly changed cellular, microscopical, biochemical, and functional aspects of the testicular tissue. Oxidative stress parameters showed supportive effects of SVF on the oxidative status of the healthy testicular tissue. Tissue and serum TOS levels of the SVF group were even lower than that of the control whereas the serum TAS level of the group was higher than that of the control. The slight increase in terms of MHDS of the SVF group can be attributed to local damage caused by the mechanical pressure of the injected volume of the cell mass. Sperm parameters were also pretty normal. In fact, no significant differences were detected between the SVF and the control group in terms of mean PCNA+, TUNEL+cell numbers, bax–Bcl-2, and CD90 levels. However, DAZL, p-p53, ATG5, and TGF-β1 levels of the SVF group were higher than those of the control group. DAZL gene expression has been located in spermatogonia, primary, and secondary spermatocytes (Pieri *et al*., 2017). DAZL has been important for meiotic division and spermatogenesis (Fu *et al*., 2015). Significant increases in the DAZL level compared to the control and BUS groups might be indicators for the inductive/restorative effects of SVF on spermatogenesis. Increased ATG-5 levels can be attributed to relatively increased autophagy and increased p-p53 levels can be attributed to the DNA damage resulting in the cellular damage of mechanical pressure of the injected SVF volume. Since TGF-β1 was reported to have both stimulatory and inhibitory effects on cellular proliferation (Roberts *et al*., 1983) and also apoptosis (Sánchez-Capelo, 2005) of spermatogenetic cells, the interpretation of increased TGF-β1/tubulin level should be made based on the clues obtained from the other parameters. Since MHDS, PCNA, and TUNEL+cell numbers, bax–Bcl-2 levels, sperm analysis, and oxidative stress parameters were not worse than those of the control group, we suggest that increased TGF-β1/tubulin level does not possess a negative impact with great importance.

To our knowledge, only one experimental study has been performed to investigate SVF on testicular injury. Zhou *et al*. (2019) reported positive effects of injected SVF cells on testicular ischemia/reperfusion injury. Inhibition of malondialdehyde levels, reduction of the damage of Leydig cells and spermatogenetic cells, restoration of hormonal homeostasis, enhanced secretion of b-FGF and stem cell factor, and promotion of spermatogenesis have been shown. In the present study, we also found SVF beneficial in the restoration of the testis tissue following busulfan-induced damage. The mean MHDS of the BUS + SVF group was not significantly better than that of the BUS group, however, tissue and serum oxidative stress levels of the BUS + SVF groups were significantly lower than those of the BUS group. Statistical differences between the BUS and BUS + SVF groups in terms of decreased TOS level together with the increased TAS level in the serum imply the antioxidant effects of SVF on not only the testes but also other internal organs affected by busulfan toxicity. Significant improvement was also detected in terms of increased healthy spermatozoa number and decreased abnormal tail number ($p < 0.001$). Increased DAZL/tubulin level vs. BUS group was consistent with better sperm analysis results. Decreased CD90/tubulin level vs. BUS group might suggest increased differentiation of stem cells into spermatogonia. Decreased ATG5/tubulin levels vs. the BUS group might be an indicator of the suppressive effect of SVF on BUS-induced autophagy. An unexpected effect of SVF on damaged testis tissue increased bax–Bcl-2 levels. We suggest that SVF shifted

the cell death pathway from necrosis to apoptosis which is more programmatic and less destructive for surrounding tissue. A significant increase in TGF-β1/tubulin level vs. BUS group ($p < 0.001$) seems to be consistent with the significant increase in bax–Bcl-2 level considering the stimulatory effect of TGF-β1 on apoptosis (Sánchez-Capelo, 2005). Decreased NF-kB also seems consistent with the increased bax–Bcl-2 level considering the role of activated NF-kB to induce the expression of gene products that block the apoptotic pathway (Yamamoto & Gaynor, 2001).

Several possible mechanisms of testicular function restoration during MSC-induced tissue regeneration have been shown. MSCs may be involved in the suppression of anti-sperm antibodies (Aghamir *et al*., 2014), can reduce factors that lead to infertility through reduction of apoptosis (Qian *et al*., 2020), can reduce oxidative stress (Abdelaziz *et al*., 2019), can stimulate testosterone production (Hsiao *et al*., 2015), can restore the damaged cells by connecting with endogenous cells (Kadam *et al*., 2019), *can* alter the expression of some spermatogenesis-related miRNAs and their target genes (Badawy *et al*., 2020). Additionally, the transplanted cells secrete growth factors such as bone morphogenetic proteins (BMPs) and transforming growth factor beta (TGF-β), which are male germ cell-inducing factors with the ability to stimulate restoration of the recipient's cellular function (Hofer & Tuan, 2016). According to the results, we obtained in this study, we suggest that SVF is beneficial in restoring damaged tissue by primarily being a multipotent cell source, by inhibiting oxidative stress and converting necrotic cell death to the apoptotic cell death.

5. Limitations

The rats were treated with human SVF containing heterogeneous human cells from a female donor. Although tissue transfer was performed between two different species, no side and immune reaction was detected as expected. Since human ASCs do not express MHC class II, we did not expect them to trigger a xenogenic immunological reaction. In humans, SVF obtained from the adipose tissue of the patient himself would be preferable, so tissue transfer would probably bring higher benefits. Nevertheless, an experimental model of the study does not exactly mimic the autologous tissue transfer.

Since the rat testes are very small, unintendedly we might have created minor mechanical damage to the tissue. In humans, the application may be easier and harmless.

Under better economic circumstances, various additional markers detecting the molecular pathways can be performed.

SVF injection plan was made by the inspiration of successful results of a few previous studies; however, different SVF injection plans in terms of injection day and the following duration period can be applied.

6. Conclusions

We suggest that SVF that is easily and quickly obtainable might be a promising effective therapeutic agent in the removal of the testicular damage induced by busulfan toxicity. In the future, clinical applications should bring higher benefits. Since SVF is the patient's own tissue, being harmless, it will offer an advantageous supportive treatment option for patients already weakened by cancer and anticancer treatment. Besides larger testicular volume in men should make the application of SVF easier and harmless.

Author contributions

Hekimoglu ER: conceptualization, methodology, resources, and writing. Esrefoglu M: writing – reviewing and editing, supervision. Pasin O: validation, formal analysis, and data curation. Karakaya Cimen FB: visualization, investigation, and resources. Elibol B: resources. Dedeakayogullari H: resources. All authors approved the final version to be submitted.

Ethical approval

Approval for the study was granted by Bezmialem Vakıf University Local Ethics Committee for Animal Experiments (Ethic Committee No.: 2021/168) and Bezmialem Vakıf University Non-Interventional Research Ethics Committee (Ethic Committee No.: E-54022451-050.05.04-33870).

Disclosure statement

No potential conflict of interest was reported by the author(s).

Funding

The project was supported by the Scientific Research Unit of Bezmialem Vakıf University (BAP No.: 20210825).

Data availability statement

All data generated or analyzed during this study are included in this published article.

References

Abarikwu, S. O., Mgbudom-Okah, C. J., Njoku, R.-C C., Okonkwo, C. J., Onuoha, C. C., & Wokoma, A. F. (2022). Gallic acid ameliorates busulfan-induced testicular toxicity and damage in mature rats. *Drug and Chemical Toxicology*, *45*(4), 1881–1890. https://doi.org/10.1080/01480545.2021.1892949

Abarikwu, S., Mgbudom-Okah, C., Onuah, C., & Ogunlaja, A. (2022). Fluted pumpkin seeds protect against busulfan-induced oxidative stress and testicular injuries in adult mice. *Drug and Chemical Toxicology*, *45*(1), 22–32. https://doi.org/10.1080/01480545.2019.1657885

Abdelaziz, M. H., Salah EL-Din, E. Y., El-Dakdoky, M. H., & Ahmed, T. A. (2019). The impact of mesenchymal stem cells on doxorubicin-induced testicular toxicity and progeny outcome of male prepubertal rats. *Birth Defects Research*, *111*(13), 906–919. https://doi.org/10.1002/bdr2.1535

Aghamir, S. M. K., Salavati, A., Yousefie, R., Tootian, Z., Ghazaleh, N., Jamali, M., & Azimi, P. (2014). Does bone marrow-derived mesenchymal stem cell transfusion prevent antisperm antibody production after traumatic testis rupture? *Urology*, *84*(1), 82–86. https://doi.org/10.1016/j.urology.2014.03.009

Andia, I., Maffulli, N., & Burgos-Alonso, N. (2019). Stromal vascular fraction technologies and clinical applications. *Expert Opinion on Biological Therapy*, *19*(12), 1289–1305. https://doi.org/10.1080/14712598.2019.1671970

Anjam, R. S., Movahedin, M., Pourbeyranvand, S., & Moula, S. J. (2007). Assessment of morphological and functional changes in the mouse testis and epididymal sperms following busulfan treatment. *Iranian Biomedical Journal*, *11*(1), 15–22.

Badawy, A. A., El-Magd, M. A., AlSadrah, S. A., & Alruwaili, M. M. (2020). Altered expression of some miRNAs and their target genes following mesenchymal stem cell treatment in busulfan-induced azoospermic rats. *Gene*, *737*, 144481. https://doi.org/10.1016/j.gene.2020.144481

Benavides-Garcia, R., Joachim, R., Pina, N. A., Mutoji, K. N., Reilly, M. A., & Hermann, B. P. (2015). Granulocyte colony-stimulating factor prevents loss of spermatogenesis after sterilizing busulfan chemotherapy. *Fertility and Sterility*, *103*(1), 270–280.e8. https://doi.org/10.1016/j.fertnstert.2014.09.023

Cai, Y., Yu, Z., Yu, Q., Zheng, H., Xu, Y., Deng, M., Wang, X., Zhang, L., Zhang, W., & Li, W. (2019). Fat extract improves random pattern skin flap survival in a rat model. *Aesthetic Surgery Journal*, *39*(12), NP504–NP514. https://doi.org/10.1093/asj/sjz112

Choi, Y.-J., Ok, D.-W., Kwon, D.-N., Chung, J-i., Kim, H.-C., Yeo, S.-M., Kim, T., Seo, H.-G., & Kim, J.-H. (2004). Murine male germ cell apoptosis induced by busulfan treatment correlates with loss of c-kit-expression in a Fas/FasL- and p53-independent manner. *FEBS Letters*, *575*(1–3), 41–51. https://doi.org/10.1016/j.febslet.2004.08.034

Corselli, M., Crisan, M., Murray, I. R., West, C. C., Scholes, J., Codrea, F., Khan, N., & Péault, B. (2013). Identification of perivascular mesenchymal stromal/stem cells by flow cytometry. *Cytometry. Part A*, *83*(8), 714–720. https://doi.org/10.1002/cyto.a.22313

Drusenheimer, N., Wulf, G., Nolte, J., Lee, J. H., Dev, A., Dressel, R., Gromoll, J., Schmidtke, J., Engel, W., & Nayernia, K. (2007). Putative human male germ cells from bone marrow stem cells. *Society of Reproduction and Fertility Supplement*, *63*, 69–76.

Erel, O. (2004). A novel automated direct measurement method for total antioxidant capacity using a new generation, more stable ABTS radical cation. *Clinical Biochemistry*, *37*(4), 277–285. https://doi.org/10.1016/j.clinbiochem.2003.11.015

Erel, O. (2005). A new automated colorimetric method for measuring total oxidant status. *Clinical Biochemistry*, *38*(12), 1103–1111. https://doi.org/10.1016/j.clinbiochem.2005.08.008

Eto, H., Ishimine, H., Kinoshita, K., Watanabe-Susaki, K., Kato, H., Doi, K., Kuno, S., Kurisaki, A., & Yoshimura, K. (2013). Characterization of human adipose tissue-resident hematopoietic cell populations reveals a novel macrophage subpopulation with CD34 expression and mesenchymal multipotency. *Stem Cells and Development*, *22*(6), 985–997. https://doi.org/10.1089/scd.2012.0442

Fu, X.-F., Cheng, S.-F., Wang, L.-Q., Yin, S., De Felici, M., & Shen, W. (2015). DAZ family proteins, key players for germ cell development. *International Journal of Biological Sciences*, *11*(10), 1226–1235. https://doi.org/10.7150/ijbs.11536

Gentile, P., Scioli, M. G., Bielli, A., Orlandi, A., & Cervelli, V. (2017). Concise review: The use of adipose-derived stromal vascular fraction cells and platelet rich plasma in regenerative plastic surgery. *Stem Cells*, *35*(1), 117–134. https://doi.org/10.1002/stem.2498

González, C. R., Muscarsel Isla, M. L., & Vitullo, A. D. (2018). The balance between apoptosis and autophagy regulates testis regression and recrudescence in the seasonal-breeding South American plains vizcacha, *Lagostomus maximus*. *PLOS One*, *13*(1), e0191126. https://doi.org/10.1371/journal.pone.0191126

Gozen, A., Demiryurek, S., Taskin, A., Ciralik, H., Bilinc, H., Kara, S., Aydin, A., Aksoy, N., & Ceylan, H. (2013). Protective activity of ischemic preconditioning on rat testicular ischemia: Effects of Y-27632 and 5-hydroxydecanoic acid. *Journal of Pediatric Surgery*, *48*(7), 1565–1572. https://doi.org/10.1016/j.jpedsurg.2012.10.074

Grasys, J., Kim, B.-S., & Pallua, N. (2016). Content of soluble factors and characteristics of stromal vascular fraction cells in lipoaspirates from different subcutaneous adipose tissue depots. *Aesthetic Surgery Journal*, *36*(7), 831–841. https://doi.org/10.1093/asj/sjw022

Guo, J., Nguyen, A., Banyard, D. A., Fadavi, D., Toranto, J. D., Wirth, G. A., Paydar, K. Z., Evans, G. R., & Widgerow, A. D. (2016). Stromal vascular fraction: A regenerative reality? Part 2: Mechanisms of regenerative action. *Journal of Plastic, Reconstructive & Aesthetic Surgery*, *69*(2), 180–188. https://doi.org/10.1016/j.bjps.2015.10.014

Hager, G., Holnthoner, W., Wolbank, S., Husa, A.-M., Godthardt, K., Redl, H., & Gabriel, C. (2013). Three specific antigens to isolate endothelial progenitor cells from human liposuction material. *Cytotherapy*, *15*(11), 1426–1435. https://doi.org/10.1016/j.jcyt.2013.06.018

Harris, W. M., Plastini, M., Kappy, N., Ortiz, T., Chang, S., Brown, S., Carpenter, J. P., & Zhang, P. (2019). Endothelial differentiated adipose-derived stem cells improvement of survival and neovascularization in fat transplantation. *Aesthetic Surgery Journal*, *39*(2), 220–232. https://doi.org/10.1093/asj/sjy130

Hofer, H. R., & Tuan, R. S. (2016). Secreted trophic factors of mesenchymal stem cells support neurovascular and musculoskeletal therapies. *Stem Cell Research & Therapy*, *7*(1), 131. https://doi.org/10.1186/s13287-016-0394-0

Hosseını, A. N., Khaki, A., Akbari, G., & Ghaffari, N. M. (2014). The effect of busulfan on body weight, testis weight and MDA enzymes in male rats. *International Journal of Women's Health and Reproduction Sciences*, *2*, 316–319.

Hsiao, C.-H., Ji, A. T.-Q., Chang, C.-C., Cheng, C.-J., Lee, L.-M., & Ho, J. H.-C. (2015). Local injection of mesenchymal stem cells protects testicular torsion-induced germ cell injury. *Stem Cell Research & Therapy*, *6*(1), 113. https://doi.org/10.1186/s13287-015-0079-0

Intarapat, S., Sailasuta, A., & Satayalai, O. (2016). Genistein causes germ cell reduction in the genital ridges of Japanese quail *Coturnix japonica* embryo. *Polish Journal of Veterinary Sciences*, *19*(1), 57–64. https://doi.org/10.1515/pjvs-2016-0008

Iwamoto, T., Hiraku, Y., Oikawa, S., Mizutani, H., Kojima, M., & Kawanishi, S. (2004). DNA intrastrand cross-link at the 5′-GA-3′ sequence formed by busulfan and its role in the cytotoxic effect. *Cancer Science*, *95*(5), 454–458. https://doi.org/10.1111/j.1349-7006.2004.tb03231.x

Kadam, P., Ntemou, E., Onofre, J., Van Saen, D., & Goossens, E. (2019). Does co-transplantation of mesenchymal and spermatogonial stem cells improve reproductive efficiency and safety in mice? *Stem Cell Research & Therapy*, *10*(1), 310. https://doi.org/10.1186/s13287-019-1420-9

Karstens, A., & Krämer, I. (2007). Chemical and physical stability of diluted busulfan infusion solutions. *European Journal of Hospital Pharmacy Science*, *13*(2), 40–47.

Lee, C., Jang, M. J., Kim, B. H., Park, J. Y., You, D., Jeong, I. G., Hong, J. H., & Kim, C.-S. (2017). Recovery of renal function after administration of adipose-tissue-derived stromal vascular fraction in rat model of acute kidney injury induced by ischemia/reperfusion injury. *Cell and Tissue Research*, *368*(3), 603–613. https://doi.org/10.1007/s00441-017-2585-0

Lin, C.-S., Xin, Z.-C., Dai, J., & Lue, T. F. (2013). Commonly used mesenchymal stem cell markers and tracking labels: Limitations and challenges. *Histology and Histopathology*, *28*(9), 1109–1116. https://doi.org/10.14670/HH-28.1109

Mehrabani, D., Hassanshahi, M. A., Tamadon, A., Zare, S., Keshavarz, S., Rahmanifar, F., Dianatpour, M., Khodabandeh, Z., Jahromi, I., Tanideh, N., Ramzi, M., Aqababa, H., & Kuhi-Hoseinabadi, O. (2015). Adipose tissue-derived mesenchymal stem cells repair germinal cells of seminiferous tubules of busulfan-induced azoospermic rats. *Journal of Human Reproductive Sciences*, *8*(2), 103–110. https://doi.org/10.4103/0974-1208.158618

Nasimi, P., Tabandeh, M. R., & Roohi, S. (2018). Busulfan-mediated oxidative stress and genotoxicity decrease in sperm of Satureja Khuzestanica essential oil-administered mice. *Systems Biology in Reproductive Medicine*, *64*(5), 348–357. https://doi.org/10.1080/19396368.2018.1449915

Nayernia, K., Nolte, J., Michelmann, H. W., Lee, J. H., Rathsack, K., Drusenheimer, N., Dev, A., Wulf, G., Ehrmann, I. E., Elliott, D. J., Okpanyi, V., Zechner, U., Haaf, T., Meinhardt, A., & Engel, W. (2006). In vitro-differentiated embryonic stem cells give rise to male gametes that can generate offspring mice. *Developmental Cell*, *11*(1), 125–132. https://doi.org/10.1016/j.devcel.2006.05.010

Nourian Dehkordi, A., Mirahmadi Babaheydari, F., Chehelgerdi, M., & Raeisi Dehkordi, S. (2019). Skin tissue engineering: Wound healing

based on stem-cell-based therapeutic strategies. *Stem Cell Research & Therapy*, *10*(1), 111. https://doi.org/10.1186/s13287-019-1212-2

Oliveira-Marques, V., Marinho, H. S., Cyrne, L., & Antunes, F. (2009). Role of hydrogen peroxide in NF-κB activation: From inducer to modulator. *Antioxidants & Redox Signaling*, *11*(9), 2223–2243. https://doi.org/10.1089/ars.2009.2601

Pak, J., Lee, J. H., Pak, N., Pak, Y., Park, K. S., Jeon, J. H., Jeong, B. C., & Lee, S. H. (2018). Cartilage regeneration in humans with adipose tissue-derived stem cells and adipose stromal vascular fraction cells: Updated status. *International Journal of Molecular Sciences*, *19*(7), 2146. https://doi.org/10.3390/ijms19072146

Panahi, M., Keshavarz, S., Rahmanifar, F., Tamadon, A., Mehrabani, D., Karimaghai, N., Sepehrimanesh, M., & Aqababa, H. (2015). Busulfan induced azoospermia: Stereological evaluation of testes in rat. *Veterinary Research Forum*, *6*(4), 273–278.

Pieri, N., Souza, A. F., Mançanares, A., Roballo, K., Casals, J. B., Ambrosio, C. E., & Martins, D. S. (2017). Immunolocalization of proteins in the spermatogenesis process of canine. *Reproduction in Domestic Animals=Zuchthygiene*, *52*(S2), 170–176. https://doi.org/10.1111/rda.12848

Qian, C., Meng, Q., Lu, J., Zhang, L., Li, H., & Huang, B. (2020). Human amnion mesenchymal stem cells restore spermatogenesis in mice with busulfan-induced testis toxicity by inhibiting apoptosis and oxidative stress. *Stem Cell Research & Therapy*, *11*(1), 290. https://doi.org/10.1186/s13287-020-01803-7

Raish, M., Ahmad, A., Ansari, M. A., Alkharfy, K. M., Aljenoobi, F. I., Jan, B. L., Al-Mohizea, A. M., Khan, A., & Ali, N. (2018). *Momordica charantia* polysaccharides ameliorate oxidative stress, inflammation, and apoptosis in ethanol-induced gastritis in mucosa through NF-kB signaling pathway inhibition. *International Journal of Biological Macromolecules*, *111*, 193–199. https://doi.org/10.1016/j.ijbiomac.2018.01.008

Roato, I., Belisario, D. C., Compagno, M., Verderio, L., Sighinolfi, A., Mussano, F., Genova, T., Veneziano, F., Pertici, G., Perale, G., & Ferracini, R. (2018). Adipose-derived stromal vascular fraction/xenohybrid bone scaffold: An alternative source for bone regeneration. *Stem Cells International*, *2018*, 4126379. https://doi.org/10.1155/2018/4126379

Roberts, A. B., Frolik, C. A., Anzano, M. A., & Sporn, M. B. (1983). Transforming growth factors from neoplastic and nonneoplastic tissues. *Federation Proceedings*, *42*(9), 2621–2626.

Rostami, A., Vakili, S., Koohpeyma, F., Jahromi, B. N., Aghajari, Z. A., Mahmoudikohani, F., Saki, F., Mahmoodi, M., Jaberi, K. R., Movahedpour, A., Khorchani, M. J., & Noroozi, S. (2022). Ellagic acid effects on testis, sex hormones, oxidative stress, and apoptosis in the relative sterility rat model following busulfan administration. *BMC Complementary Medicine and Therapies*, *22*(1), 170. https://doi.org/10.1186/s12906-022-03650-w

Rufini, A., Tucci, P., Celardo, I., & Melino, G. (2013). Senescence and aging: The critical roles of p53. *Oncogene*, *32*(43), 5129–5143. https://doi.org/10.1038/onc.2012.640

Sánchez-Capelo, A. (2005). Dual role for TGF-β1 in apoptosis. *Cytokine & Growth Factor Reviews*, *16*(1), 15–34. https://doi.org/10.1016/j.cytogfr.2004.11.002

Siregar, S., Sasongko Noegroho, B., Adriansjah, R., Mustafa, A., & Wijayanti, Z. (2021). Intratesticular human adipose-derived stem cell (hADSC) transplantation decreased oxidative stress in testicular torsion model of Wistar rat. *Research and Reports in Urology*, *13*, 1–8. https://doi.org/10.2147/RRU.S283861

Speidel, D. (2015). The role of DNA damage responses in p53 biology. *Archives of Toxicology*, *89*(4), 501–517. https://doi.org/10.1007/s00204-015-1459-z

Taslidere, E., Esrefoglu, M., Tok, O. E., Taslidere, B., & Bulut, H. (2022). Effects of melatonin on both testicular regeneration and recovery of spermatogenesis in busulfan-treated rats. *Brazilian Journal of Pharmaceutical Sciences*, *58*. https://doi.org/10.1590/s2175-97902022e20945

Tiryaki, T., Canikyan, S., Koçak, P., Cohen, S., Sterodimas, A., Schlaudraff, K., Scheflan, M., & Hollands, P. (2021). Adipose-derived stromal vascular matrix (SVM): A new paradigm in regenerative medicine. *CellR4*, *9*, e3060.

Vahdati, A., Fathi, A. R., Nasimi, P., & Saki, G. (2015). Busulfan induces apoptotic and cytotoxic effects on testis and epididymal sperm of adult male mouse following low dose treatment. *International Journal of Biology*, *5*, 70–78.

van Dongen, J. A., Harmsen, M. C., & Stevens, H. P. (2019). Isolation of stromal vascular fraction by fractionation of adipose tissue. *Methods in Molecular Biology*, 1993, 91–103.

Xu, L.-L., Liu, M.-L., Wang, J.-L., Yu, M., & Chen, J.-X. (2016). Saligenin cyclic-o-tolyl phosphate (SCOTP) induces autophagy of rat spermatogonial stem cells. *Reproductive Toxicology*, *60*, 62–68. https://doi.org/10.1016/j.reprotox.2016.01.004

Yamamoto, Y., & Gaynor, R. B. (2001). Role of the NF-kB pathway in the pathogenesis of human disease states. *Current Molecular Medicine*, *1*(3), 287–296. https://doi.org/10.2174/1566524013363816

Yasuda, K., Ozaki, T., Saka, Y., Yamamoto, T., Gotoh, M., Ito, Y., Yuzawa, Y., Matsuo, S., & Maruyama, S. (2012). Autologous cell therapy for cisplatin-induced acute kidney injury by using non-expanded adipose tissue-derived cells. *Cytotherapy*, *14*(9), 1089–1100. https://doi.org/10.3109/14653249.2012.693157

Zhou, L., Song, K., Xu, L., Zhao, F., Tian, H., Zhou, C., Xu, Z., Ge, Y., Wu, R., & Jia, R. (2019). Protective effects of uncultured adipose-derived stromal vascular fraction on testicular injury induced by torsion–detorsion in rats. *Stem Cells Translational Medicine*, *8*(4), 383–391. https://doi.org/10.1002/sctm.18-0063

Zimmerlin, L., Donnenberg, V. S., Rubin, J. P., & Donnenberg, A. D. (2013). Mesenchymal markers on human adipose stem/progenitor cells. *Cytometry. Part A*, *83*(1), 134–140. https://doi.org/10.1002/cyto.a.22227